Arabian Journal for Science and Engineering (2022) 47:15989–16000
https://doi.org/10.1007/s13369-022-06780-y

RESEARCH ARTICLE-MECHANICAL ENGINEERING

Mechanical and Tribological Studies on AZ91E Magnesium Alloy Reinforced with Lanthanum Hexa-aluminate Nanoparticles

Naga Venkata Sai Ram Yellapragada[1,2] · Tara Sasanka Cherukuri[2] · Prabakaran Jayaraman[1]

Received: 1 August 2021 / Accepted: 2 March 2022 / Published online: 18 April 2022

Abstract
The present work is triggered on the processing and characterization of magnesium AZ9E/LHA composites. Lanthanum hexa-aluminate (LHA) nanoparticles are prepared by chemical precipitation and filtration technique followed by characterization studies conducted through X-ray peak profile analysis and field emission scanning electron microscopy supported by energy-dispersive spectroscopy (EDS). Later on lanthanum hexaluminate powders (LHA) were presented as a candidate process to disseminate in the AZ91E alloy. The stir casting procedure was used to manufacture magnesium AZ91E/LHA composites. The effects of varying the reinforcement weight fraction on particle distribution, particle–matrix interfacial interactions, physical, tribological and mechanical properties were investigated. The existence of components and a uniform distribution of particles in the composite were revealed by SEM and EDS examination. The mechanical characteristics of both reinforced and unreinforced composites were assessed and reported. An increment of 18.61% micro-hardness and 17.43% in tensile strength is observed. The worn surfaces of all fabricated composites were examined using scanning electron microscopy for understanding the wear mechanism.

Keywords AZ91E · LHA · Wear · Tribology · Mechanical behaviour

1 Introduction

The world is changing quickly, and as a result, the demand for lightweight materials is increasing day by day. This leads to trend in automobiles to substitute Al and Mg for conventional steel and cast irons for the stringent requirements like increased fuel economy and emissions. Alloys of magnesium find better usage in industrial applications, especially in the automotive industry because of its lightweight (75% less than steels and 30% less than Al), better mechanical properties compared to aluminium alloys or steels. Because of its low density, magnesium is employed as a matrix material in MMCs. These magnesium matrix composites (MMCs) are found to be one of the best alternatives for meeting the increasing need for lightweight structural materials in the automotive, aerospace industries and various other domains [1–5]. Despite this, its poor thermal stability and wear resistance prevent it from being used as cylinder liners and pistons in automobile engines [6]. To overcome this, hard ceramic particles, especially at nanoscale, are disseminated in the Mg matrix to improve the wear resistance. Strengthening the metal matrix with hard micro-/nano-sized ceramic particles, as in the traditional Archard idea, can improve both mechanical behaviour (hardness, strength) and tribological (wear resistance) performance [7, 8].

In the recent past, a lot of work has been carried out by various researchers to enhance the usage of magnesium alloys as a substitute to conventional monolithic alloys [9]. Out of many Magnesium alloys, AZ91E (9Al-1Zn-0.2Mn) is the most prevalent alloy having optimal combination of good castability, enhanced mechanical strength and better ductility. However, the safe use of AZ91E is constrained to 1200C. To overcome this constraint, many researchers reinforced the micro- and nanosize powders to AZ91E alloys. Saranu et al. [10] investigated the effects of silicon carbide nanoparticles and fly ash on the mechanical characteristics of the magnesium AZ91E alloy. They found that adding both a hard reinforcement (e.g. SiC) and a soft reinforcement (e.g. fly ash) to magnesium composites significantly enhances mechanical properties such as tensile strength and hardness. However, grain refinement caused by the addition

✉ Naga Venkata Sai Ram Yellapragada
ynvsr@rvrjc.ac.in

1 Annamalai University, Chidambaram, India

2 R.V.R. & J.C. College of Engineering, Guntur, India

of reinforcing particles reduced the fracture toughness and elongation of magnesium composites. Deng et al. [11] stated that the SiCp/AZ91 composites exhibit a significant hike in micro-hardness in contrast to the unreinforced AZ91E alloy. Researchers also studied the elevated temperature and creep behaviour of magnesium alloys. Mao et al. [12] studied the usage of Mg–Al alloy for elevated temperature applications, whereas Yang et al. [13] studied the creep behaviour of Mg–Al–RE alloy. Sameer et al. [14] studied the fatigue strength of Ni-coated alumina composites in AZ91E alloy.

Out of all most important issue has been the wear resistance of magnesium alloys, which has been the fascinating subject of interest to date. To enhance wear behaviour of magnesium alloys, many researchers dispersed the ceramic particles into the magnesium alloys. They reported that wear when compared to unreinforced Mg alloys, alumina exhibits improved hardness and strength and also contributes to good wear resistance. Zeng et al. [15] investigated the tribological behaviour of Al_2O_3–MoO_2–SiO_2 Composite Ceramic Coating and found that the morphology and structure change when molybdate is added to the electrolyte. The surface features and hardness of the coatings have a significant impact on tribological behaviour.

Chen et al. [16] reported the behaviour of wear for AZ91 alloy by varying the applied loads and sliding speeds. Aung et al. [17] investigated the influence of low sliding speeds on wear behaviour of AZ91 Mg alloy. Lim et al. [18] look overed the wear behaviour under dry sliding conditions using SiC as reinforcement in magnesium MMCs using a pin-on-disc tribometer against a hard steel counter-face under variable normal loads (10 N, 30 N) and sliding velocities (0.20 to 5 m s−1), respectively. Lim et al. [19] in their study reported the wear mechanisms involved in magnesium matrix composites with 1.11 vol. % Al_2O_3 particles. Under a constant load of 10 N, with increase in amount of reinforcement of alumina and varying the sliding velocities in a range (1–10 m/s), it is observed that wear resistance is enhanced.

Rare earth elements (REEs) that acquire peculiar physical and chemical properties are being used for multiple domains like electronics and aerospace fields, etc. Kaveh Meshinchi Asl et al. [20] investigated the behaviour of wear for AZ91 alloy at room temperature with varied percentage of cerium (1%, 2%, 3%). Lanthanum hexa-aluminate ($LaAl_{11}O_{18}$) is truncated as LHA which belongs to the rare earth aluminate family with magnetoplumbite structure with a unique stoichiometry and it is the key compound formed in La_2O_3–Al_2O_3 system and it is used as a novel material in thermal barrier coating (TBC's) [21, 22]. The results of literature survey indicate a lot of work has been carried out using various ceramic materials like silicon carbide, boron carbide alumina with increasing various weight fractions but no attempts have been made to study the LHA as reinforcement in magnesium AZ91E alloy. So present paper going to take step forward to find the mechanical and wear behaviour of AZ91E/LHA composites for different weight fractions.

2 Materials and Methods

2.1 Powder Preparation and Characterization

2.1.1 Preparation of Powders

Alumina powder, lanthanum oxide, aluminium nitrate, ammonium carbonate(), and citric acid are used in this research. Mincometsal Pvt. Limited in Bengaluru provided the lanthanum oxide, while Krish Met Tech Pvt. Limited in Chennai provided the high grade alumina. National Scientific Products, Guntur, provided the supporting chemicals such as aluminium nitrate, ammonium carbonate, and citric acid. Lanthanum hexaluminate ceramic (LHA) powders were synthesized using chemical precipitation and filtration method and process is depicted in Fig. 1. These LHA nanoparticles are prepared using the following stoichiometric reactions Eqs. (1) and (2).

$$La_2O3 + 6\,HNO_3 + 9H_2O \rightarrow 2\left[La\,(NO_3)_3.6\,H_2O\right] \quad (1)$$

$$2\left[La\,(NO_3)_3.6H_2O\right] + 22\,Al\,(NO_3)_3.9\,H_2O \rightarrow 2\,LaAl_{11}O_{18} + 72\,HNO_3 + 174\,H_2O \quad (2)$$

2.1.2 XRD Analysis of Powders

XRD data for prepared powders are extracted using the MINIFLEX 600 machine in a range from 3 to 90 degrees in 0.02 degree steps, and peak analysis is performed using Match software. As the phases between Lanthanum and Alumina become more distinct, it indicates that the powders have been effectively blended. From Eq. 2, the end product of chemical synthesis was observed to be lanthanum aluminate($AlLaO_3$), lanthanum hexa-aluminate($Al_{11.5}La_{0.85}O_{18.5}$) and depicted in XRD peak analysis (Fig. 2). The same was confirmed with JCPDS cards 31-0022 and 33-0699. The formation of a hexagonal structure with a magneto plumbite phase was seen, which is supported by the literature [24].

The prevalence of tiny sized crystals in the samples is visible from the peak widening of the XRD pattern. The strong diffraction peaks indicate that the produced LHA particles have good crystallinity.

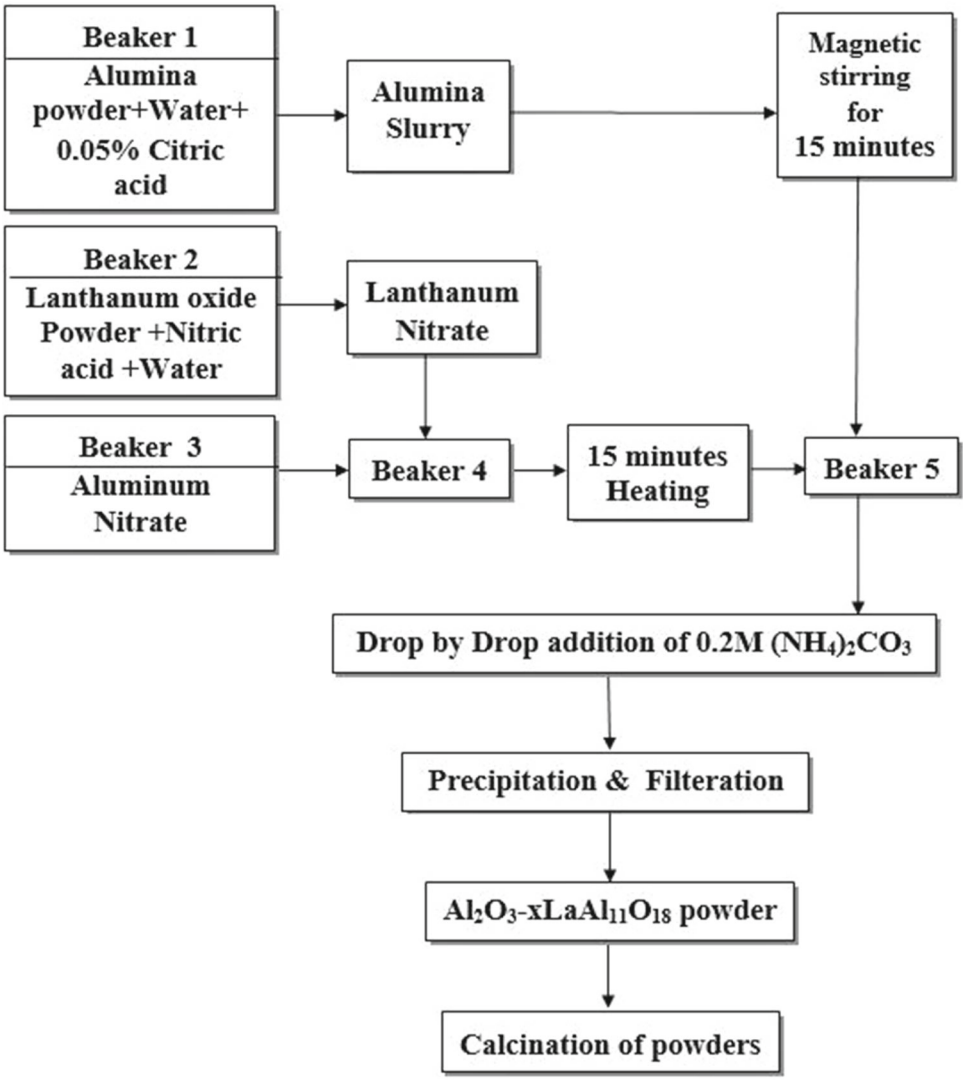

Fig. 1 Flow chart for preparation of LHA powders [23]

2.1.3 SEM Analysis of Powders

Figure 3a shows that the approach used here is successful in creating nanoparticles that are almost identical in size and form. The particle sizes of spherical-shaped LHA nanoparticles ranged from 64 to 88 nm with a mean particle size of 76 nm, according to FESEM analysis. Figure 3b shows the EDS analysis of the manufactured powder, which revealed that the sample largely comprises aluminium and lanthanum, revealing the process's primary constituent materials.

2.2 Fabrication of Composites

In the study, magnesium AZ91E is selected as matrix materials as out of various magnesium alloys AZ91E has emerged as best material in view of automotive applications [25]. The chemical composition of AZ91E magnesium alloy is shown in Table 1.

Composites are fabricated using mild steel die in an induction furnace under a cover of flux (20% KCl, 15% MgO, 15% CaF_2, 50% $MgCl_2$ by weight) and with a high purity (99.9%) argon gas at RVR&JC, Guntur. The preheated LHA powders (avg. size 75 nm) enfolded in an aluminium foil were drowned below the melt, as per the wt% calculated. After that, the mixture was agitated for 5 min with a three-blade stirrer at a rotation speed of 350 rpm before being poured into a mild steel mould with dimensions of Ø15 mm × 150 mm in height. The present study focuses on Magnesium AZ91E alloy reinforced with LHA ceramic powder additions increased from 2 to 8%wt LHA at 2%wt interval. Figure 4 depicts the stir casting set-up used for fabrication of composites.

2.3 Porosity Measurement

Equation (3) is used to calculate porosity in relation to theoretical and experimental densities [28]. The theoretical

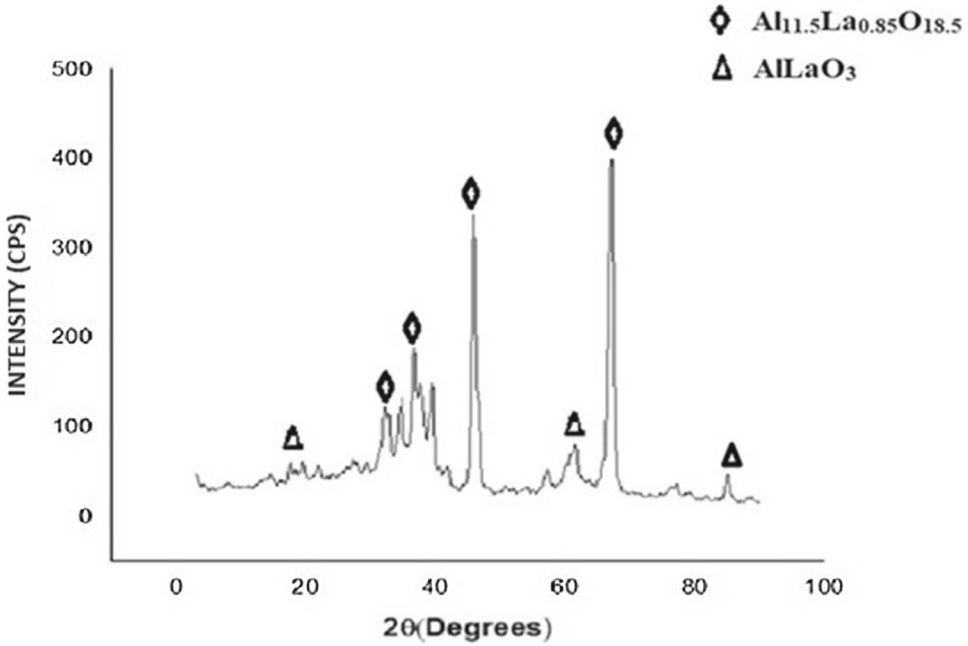

Fig. 2 XRD analysis of prepared LHA powder

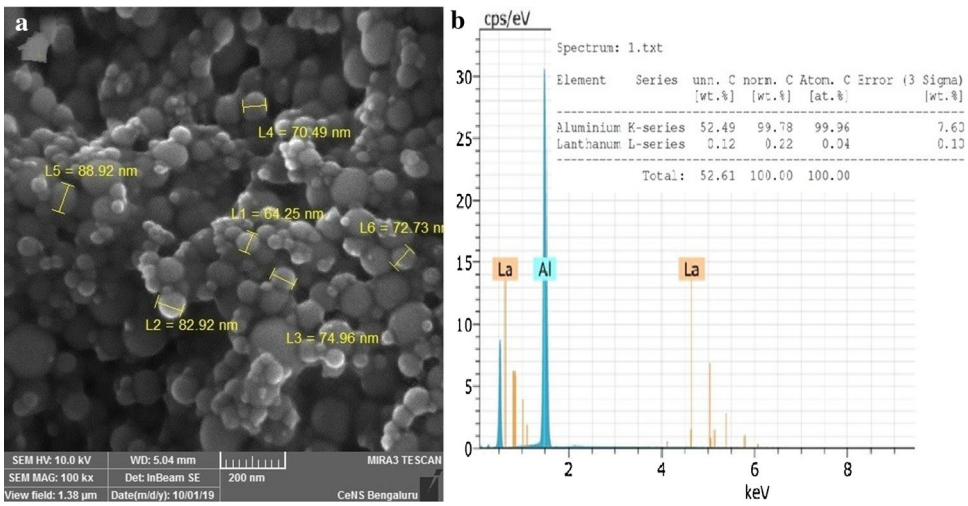

Fig. 3 **a** SEM image of prepared LHA powder **b** EDX analysis of LHA powder

Table 1 Chemical composition of AZ91E magnesium alloy used in experiments (wt. %) [26]

Element	Al	Zn	Si	Mn	Cu	Ni	Fe	Mg
Weight%	9.01	0.82	0.01	0.22	0.001	0.002	0.0017	Bal

density of LHA particle was measured to be 4.01 g/cc. With deionized water as the dipping fluid, the densities of composites were assessed using the Archimedes principle. The samples were surface finished and the weights were calculated with an electronic balance. Eight density readings were collected for each sample, and the mean value was calculated.

$$\%\text{porosity} = 1 - \left(\frac{\text{measure density}}{\text{theoretical density}}\right) X100 \quad (3)$$

2.4 Mechanical Properties Assessment

In terms of micro-hardness and tensile characteristics, the mechanical behaviour of the composite with varying weight percentages of reinforcements was studied. The influence of reinforcement and its effect on hardness was investigated through hardness tests. Micro-hardness was estimated using a Vickers hardness test (Model: HVS 1000B) for a load of 100 gf and a loading time of 15 s. For each sample, to estimate hardness, eight readings are taken and mean of these eight

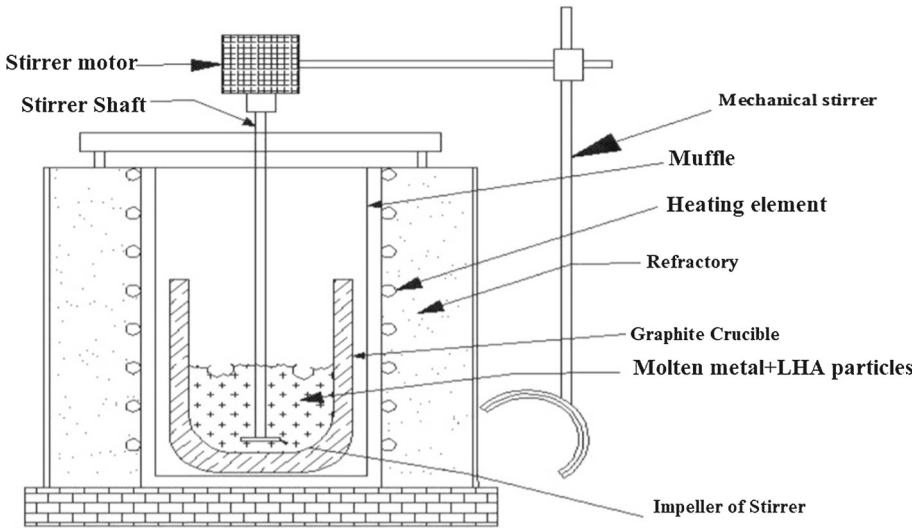

Fig. 4 Stir casting set-up [27]

Table 2 Specifications of the machine and parameters taken constant during wear test

Model	Wear and Friction Monitor TR-20
Pin material	MI.MII,MIII,MIV,MV
Pin dimensions	Φ8 mm × 50 mm length
Sliding speed (m/s)	3.40(650 rpm), 5.23(1000 rpm),
Wear test time (minutes)	For 3.40 m/s = 14.6, 5.23 m/s = 9.5
Wear track diameter (m)	0.1
Normal load applied (N)	10, 50
Disc material	EN31 steel
Normal load range of the machine (N)	4.9 to 200
Wear measurement range of the machine	0 to 2000 micro metres

Table 3 Porosity calculations of AZ91E alloy and prepared composite

Material	Theoretical density gcm^{-3}	Experimental density gcm^{-3}	% Porosity
AZ91E	1.810	1.804	0.331
AZ91E + 2 wt% LHA	1.855	1.837	0.970
AZ91E + 4wt% LHA	1.900	1.852	2.520
AZ91E + 6 wt% LHA	1.945	1.878	3.440
AZ91E + 8 wt% LHA	1.991	1.881	5.470

readings is taken as hardness value. As per ASTM_B557 Standard, tensile test was conducted on UTN 40, for each composition, three readings were recorded.

2.5 Wear Set Up

The dry sliding wear characteristics of prepared Magnesium matrix composites have been carried out as per ASTM G99-05 standards using wear measuring machine (TR-20) with computerized data acquisition system and the schematic layout in shown in Fig. 5. The specifications and the parameters considered for experimentation are given in Table 2. During the test, the load was applied to the pin, such that pin makes the contact with the disc made of EN32 (58–60 HRC). The specimens were removed from the machine after passing through the specified sliding distance. The samples were rinsed in acetone and wear is predicted in terms of weight loss of the pin. The wear loss of the composite was determined by the variation in weight measured before and after each examination. % of reinforcement (R), normal loads (L), sliding distance (D) and sliding velocity (S) were examined as a function of the wear (W, μm) and frictional force (FF, N) of LHA reinforced magnesium AZ91E alloy composites.

3 Results and Discussion

3.1 Density and Porosity

In contrast to theoretical density and measured density, porosity is estimated using Eq. (3) and given in Table 3. The low porosity suggests that the casting was successful. It has been observed that as the wt per cent of reinforcement increases, the porosity increases. Sameer et al. [30] and Aravindan et al. [31] found the similar tendency for

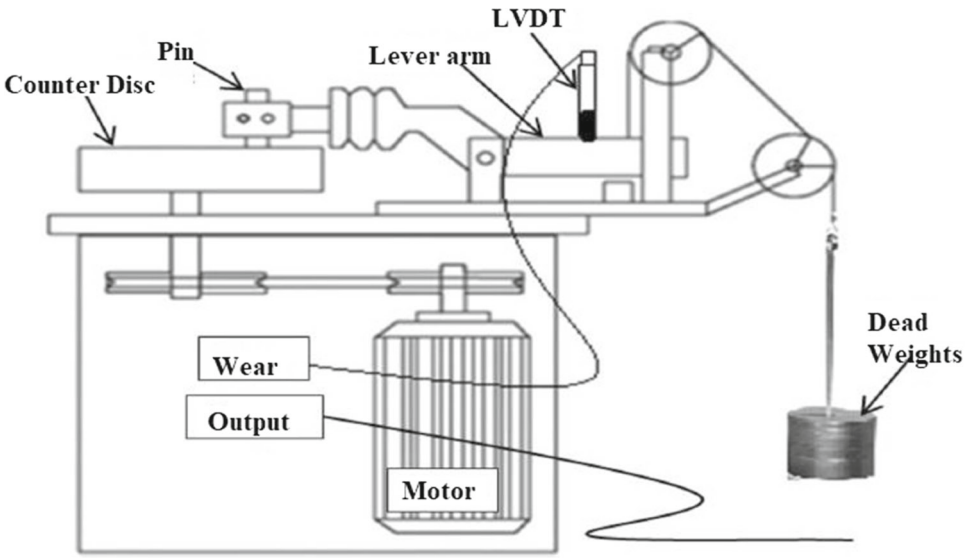

Fig. 5 Pin-on-disc tribometer [29]

AZ91E/Nanoalumina composites and AZ91D/SiC composites. The presence of agglomerations, incoherence during stirring and pouring into the moulds may be the reason behind gases entrapment which caused larger porosity value at higher percentages of reinforcements.

3.2 Microscopy Results

Electrical discharge machining was used to cut the specimens with dimensions of 20 mm × 20 mm × 2 mm from homogeneous AZ91E/LHA composites to analyse the microstructure. Before examination, the samples were polished thoroughly to prevent fine scratches and etched for 5 s with an acetic-picric solution. Microstructure analysis of the produced composites was analysed using SEM (Model: VEGA3, TESCAN) coupled with EDX (Model: BRUKER nano, GmbH, D-12489) to show the distribution of lanthanum Hexa-aluminate particles inside AZ91 matrix microstructures. A detailed look at the microstructure in Fig. 6 using SEM and EDS reveals that it is made up of primary α-Mg with a separate intermetallic eutectic phase β-$Mg_{17}Al_{12}$. These precipitates were hard and brittle, and they, along with Alumina particles, contributed to the alloy's hardness [32]. The uniform distribution (Fig. 7) of LHA may be depicted from the micrographs for 6% wt LHA thereafter addition of further reinforcement caused aggloromations and seen in Fig. 8.

3.3 Mechanical Properties

Due to their low strength and stiffness, alloys of magnesium have limited applicability in multiple domains. Alloys of magnesium and its composites with improved mechanical characteristics can overcome such challenges. This section examines and reports the hardness, tensile properties which include ultimate tensile strength, elastic modulus (stiffness), yield strength and ductility of AZ91E and processed composites.

Table 4 Hardness results

Material	Micro-hardness(HV)
AZ91E	78.3 ± 5
AZ91E + 2 wt% LHA	81.5 ± 3
AZ91E + 4wt% LHA	89.3 ± 4
AZ91E + 6 wt% LHA	96.2 ± 2
AZ91E + 8 wt% LHA	92.1 ± 5

3.3.1 Hardness

Table 4 shows micro-hardness values for various reinforcing weight percentages. When compared to the base alloy, micro-hardness levels grow in tandem with the percentage of reinforcement. The pure AZ91 alloy has a hardness value of 78.3 ± 5 VHN. Composites reinforced with LHA particles at 2 wt% have the lowest hardness (81.5 ± 3VHN), while composites reinforced with LHA particles at 6 wt% have the highest (96.2 ± 2VHN). When comparing composites to unreinforced magnesium alloy, the maximum rise in hardness is found to be 18.61%.

The hardness enhancement was attributable to the presence of hard LHA particles, which help the material's load bearing capacity while also limiting matrix deformation by restricting dislocation mobility. Because of the poor distribution of LHA nanoparticles, the increase in reinforcement leads in a decrease in hardness after 6% of weight fraction. It

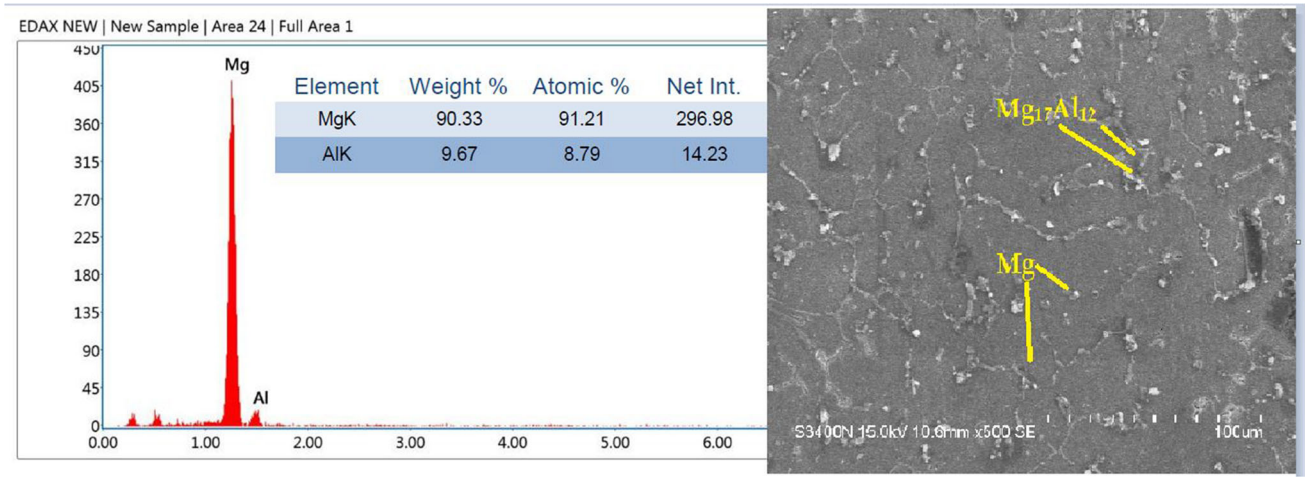

Fig. 6 SEM/EDX analysis of AZ91E alloy

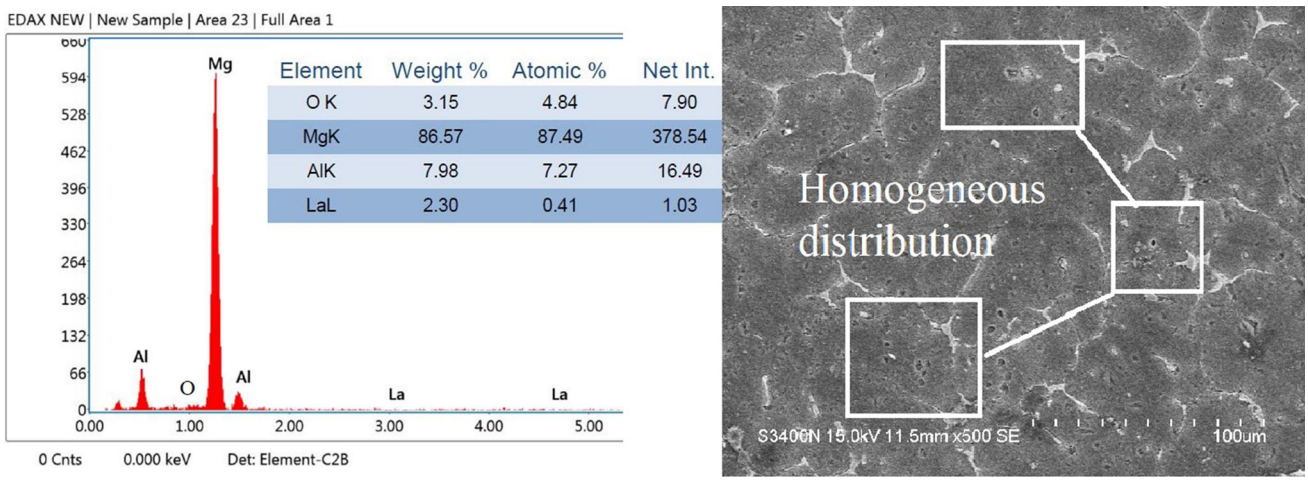

Fig. 7 SEM/EDX analysis of AZ91E/6 wt %LHA alloy

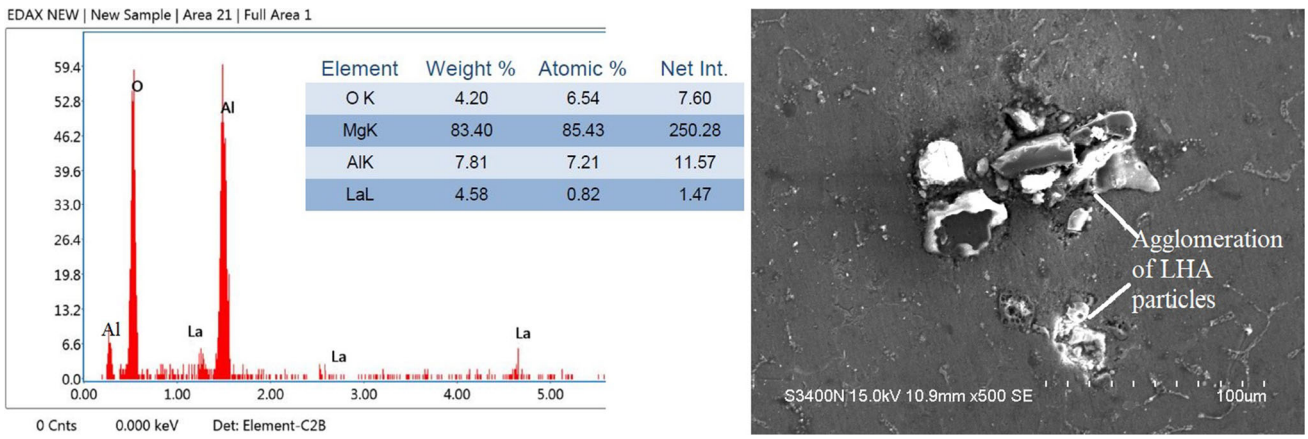

Fig. 8 SEM/EDX analysis of AZ91E/8 %LHA alloy

is also worth noting that the hardness trend seen in this work resembles the work reported by Poddar et al. [33].

3.3.2 Yield Strength

As the volume fraction of hard LHA particles in the AZ91E composite increases, the yield strength of the composites increases. The interfacial bond between the reinforcement and matrix is due to the size and shape of the particle leading to composite strength [34, 35]. The load applied can be shifted from the magnesium alloy to hard LHA particle with the bonding between the matrix and the reinforcement is sufficiently strong. The comparatively magnesium alloy matrix is protected by the increased strength of LHA particles. The yield strength of the base material (0.2 per cent offset) is 94 MPa, while the highest yield strength recorded for the 6 wt% fraction is 126 MPa (Fig. 11). It was obvious that as the volume per cent increased, more loads could be carried to the reinforcement, resulting in better yield strength.

3.3.3 Tensile Strength

The major goal in producing the composite material is to make it extremely strong. When a tensile load is applied, severe internal stresses are created, which can lead to a localized failure if the local stress exceeds the material's strength. Distribution of stress is borne uniformly by the reinforcing particles, which lags the creation of localized damage [33]. It can be shown that increasing the LHA volume percentage causes the stress distribution to shift to the hard phase, which enhances the tensile strength. Figure 9 depicts the yield and tensile strength variations for the alloy and composite. The tensile strength of as casted AZ91E is 161 MPa, 172 MPa, 183 MPa, 195 MPa, 183 MPa for 2%, 4%, 6% and 8% reinforcement, respectively.

When compared to cast AZ91, it is obvious that composites have a higher tensile strength. Because of defects formed around the LHA particles may result in delamination of the interface and a drop in ultimate tensile strength in the composites as there is an increment in the LHA content. Sameer et al. found the same thing with the AZ91E alloy, which uses nanoalumina as reinforcement [30]. The reaction of AZ91E with LHA ceramic powders results in the production of hard layers if the reinforcement percentage reaches a level. Although these layers enable a bonding between alumina and magnesium alloy, they are not tough enough to transmit loads and so they frequently promote reduction in composites tensile properties [33].

3.3.4 Ductility

As illustrated in Fig. 5b, the % of elongation has decreased from 3.08 to 1.94. The reduction in ductility may be due to nucleation of voids as reinforcement percentage increased. The high stress concentration at the cracked particle's tip may also contribute to the reduction in composites ductility value. As lanthanum hexa-aluminate powders which are derived from alumina powder may act as stress concentrators and leading to particle aggloramations. Due to aggloramated particles, the stress value increases dramatically, resulting in detachment of matrix and reinforcement materials.

3.3.5 Modulus of Elasticity

Stiffness is the rigidity that can be estimated by modulus of elasticity of the composite. As predicted, addition of LHA particles to base AZ91E alloy results in betterment of modulus. The tiny and strong reinforcing particles distributed throughout the matrix inhibit dislocation motion and strengthen the magnesium alloy composite. Young's modulus is affected by the percentage of reinforcement, matrix distribution, shape, and size [31, 33]. Halpin–Tsai equation (Eq. 4) and rule of mixtures (Eq. 5) are used to determine the modulus of elasticity. For continuous reinforcements, the Rule of Mixtures (ROM) expression is preferable, whereas the other is best for discontinuous reinforcements [31].

By using equation suggested by Halpin–Tsai

$$E_c = \frac{E_m(1 + 2S * q * V_r)}{(1 - q * V_r)} \tag{4}$$

where $q = \left[\frac{\frac{E_p}{E_m} - 1}{\frac{E_p}{E_m}}\right] + 2S.$

The Rule of Mixtures Equation:

$$E_c = E_m V_m + E_r V_r \tag{5}$$

The mixing rule is clear and simply concerns volume fraction and modulus of elasticity, whereas Halpin–Tsai also considers the aspect ratio of the reinforcement particle. For all of the reinforcements, elastic modulus was computed using both approaches. The measured and estimated elastic modulus for the fabricated composites with various reinforcements are depicted in Fig. 10.

3.4 Wear Behaviour

The dry sliding wear tests were carried out under loads (10 N, 50 N), Speeds (650 rpm, 1000 rpm) at constant sliding distance of 3000 m. The wear is recorded in relation with time and monitored continuously using computerized data acquisition system for all composites. Increment in LHA content in AZ91E magnesium composites will significantly decrease the wear rate compared to base alloy. Qing-ju [36] investigated the outcomes of graphite particulates on tribological behaviour of AZ91 magnesium alloy composites in a dry

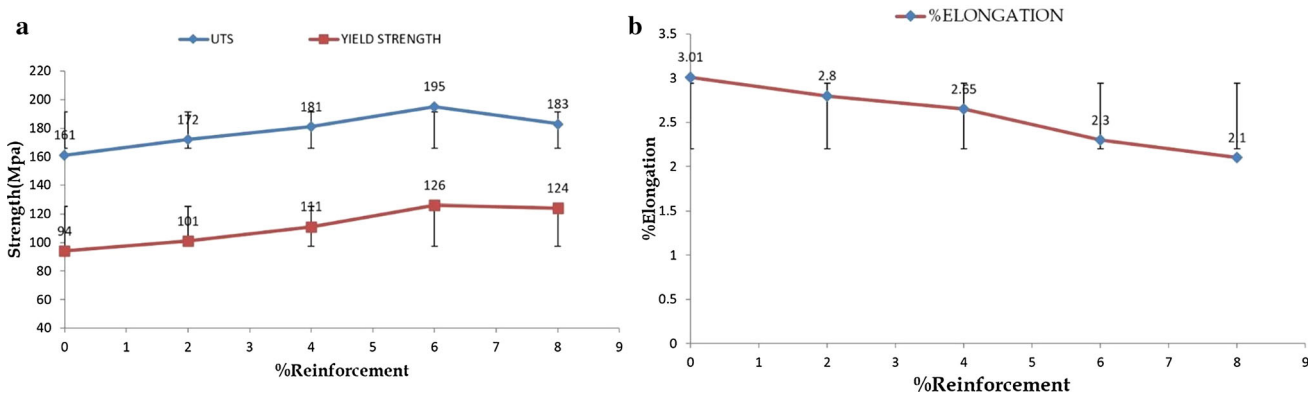

Fig. 9 **a** Variation in yield and tensile strength with reinforcement **b** Variation in elongation with reinforcement

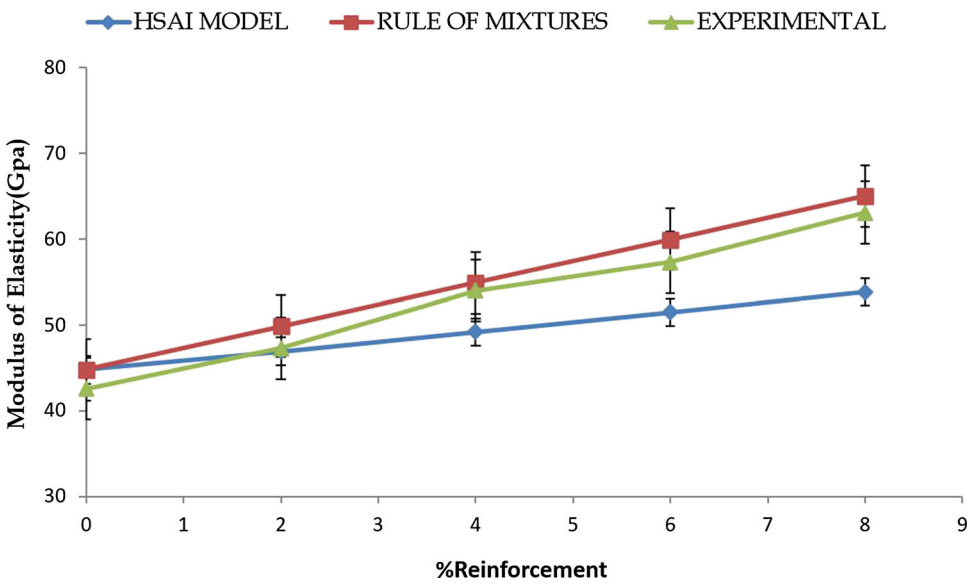

Fig. 10 Representation of modulus of elasticity using experimental, ROM and Halpin–Tsai model

sliding environment and reported that resistance of wear in composite shows superior behaviour in relation to base alloy. Mondal and Kumar [37] searched the wear behaviour of saffil short fibres and SiC particles reinforced creep-resistant AE42 magnesium alloy composites and reported that with increment in load, the rate of wear is also increased for both the composites and alloy. As the applied load increased, the wear mechanism changed from abrasive wear to particle cracking induced delaminating wear, which led to increased wear severity [38].

Figures 11 and 13 depict the Time versus Wear plots for load 10 N, Speed = 650 rpm and load = 50 N, Speed = 1000 rpm maintaining a constant sliding distance of 3000 m. At a lower sliding velocity and applied load, oxidation dominated the wear mechanism. Microcracks are observed in Fig. 12 due to abrasive wear because of surface deformation in the sliding direction. More number of parallel ridges and grooves have also been found parallel to the sliding direction. These characteristics are typical observations of abrasive wear (Fig. 13). When hard particles present in the gap between pin and the disc plough the pin surface, removing small fragments on the surface of material and generating wear [39].

As the load and speed were increased, a combination of oxidation, adhesion, abrasion, and delamination occurred. When the applied load reached 50 N, the wear mechanism abruptly changed from abrasion to delamination, as shown in Fig. 14. The abrupt changes are caused by the presence of agglomerated LHA particles or by blow holes in the composite samples. The material is detached from the surface of pin in the form of bulges or hard particles on the surface, leading to ploughing of the surface [39, 40]. The deep grooves and delamination seen at high speeds and with 50 N normal loads suggest that cutting is the form of wear. [41] This is due to the hard asperities penetrating the pin surface with minimum material displacement on either sides of the grooves during sliding.

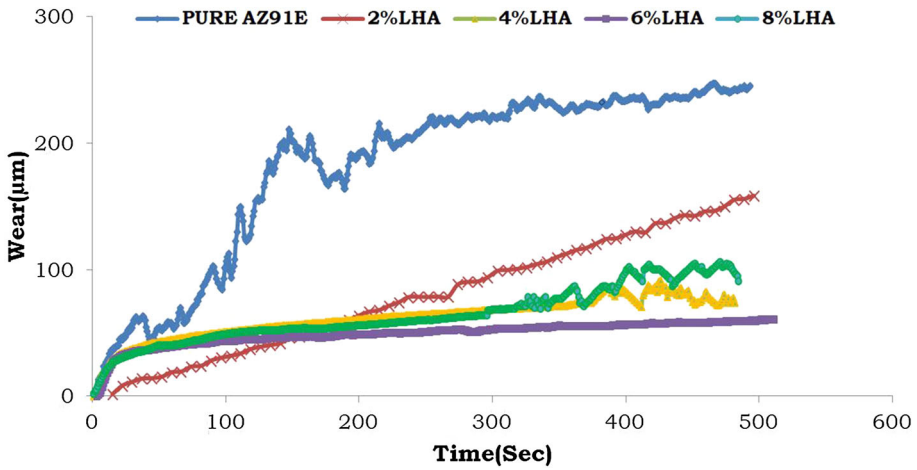

Fig. 11 Time versus wear for load = 10 N at $N = 650$ rpm

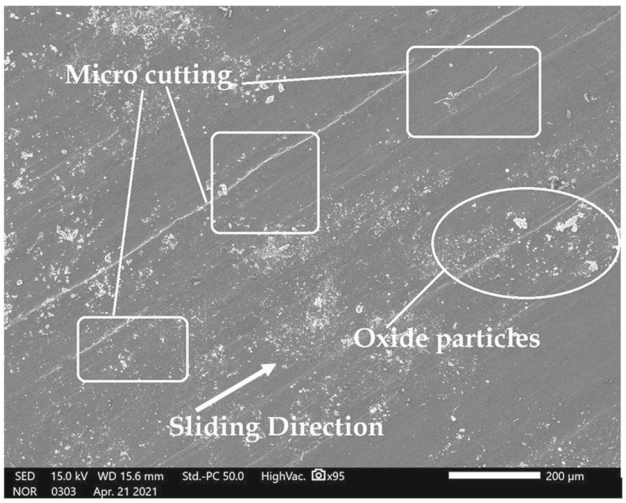

Fig. 12 SEM of worn surface for load = 10 N at $N = 650$ rpm

4 Conclusions

The following conclusions were made based on the experimental results:

- Using stir casting technique, magnesium AZ91E/LHA composites were successfully fabricated with various percentages by weight ranging from 2 wt% to 8 wt% at 2 wt% interval. As a result of proper stirring, homogeneous distribution of LHA nanoparticles in the matrix material is obtained.
- Mechanical behaviour (hardness, yield and tensile strengths) of the composites was found to increase with increased nanoLHA up to 6%, then decreased with the further addition of nanoparticles on account of aggloromations.
- From the results, 6 wt% reinforced composites has dominated the other reinforcements in giving better mechanical properties due to uniform distribution over the matrix. An increment of 18.61% micro-hardness and 17.43% in tensile strength is observed.

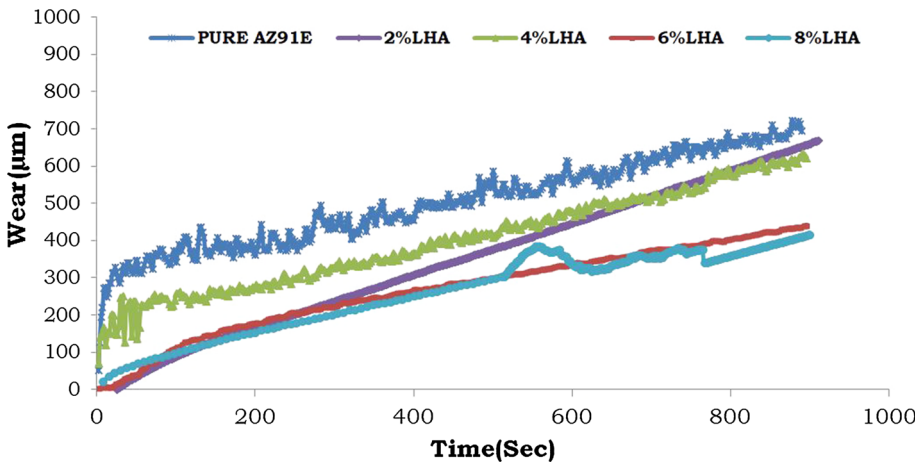

Fig. 13 Time versus wear for load = 50 N at $N = 1000$ rpm

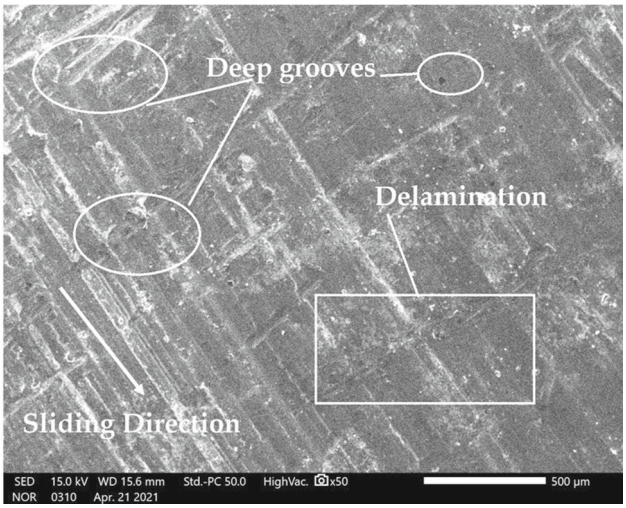

Fig. 14 SEM of worn surface for load = 50 N at $N = 1000$ rpm

- Using pin-on-disc apparatus, dry sliding tests of AZ91E alloy and its composites against a EN32 steel counterpace were carried out for loads 10 N, 50 N, respectively. Abrasion and delamination occurred in the processed composites. Abrasive wear is activated at lower load (10 N,650 rpm), whereas delamination is seen at high loads(50 N,1000 rpm)
- Improvement in wear behaviour is observed under varying normal loads and low sliding velocities. The wear rate rises suddenly above a critical load. Lanthanum hexa-aluminate particles aid in delaying the transition from moderate to severe wear.

Declarations

Conflict of interest No potential conflict of interest was reported by the authors.

References

1. Kumar, N.; Soren, S.: Effect of aluminium in magnesium alloy fabricated through the squeeze casting process. In: Proceedings of Fourth International Conference on Inventive Material Science Applications, pp. 113–119. Springer, Singapore (2022)
2. Wang, X.; Su, Y.; Guo, L.; Liu, Y.; Li, H.; Ren, H.: Research progress of heat resistant magnesium alloys. In: Journal of Physics Conference Series, Vol. 2160, p. 012015. IOP Publishing, Bristol (2022)
3. Kumar, D.; Phanden, R.K.; Thakur, L.: A review on environment friendly and lightweight Magnesium-Based metal matrix composites and alloys. Mater. Today Proc. **38**, 359–364 (2021)
4. Sowjanya, C.; Nagabhushanao, V.; Pavani Sri Kavya, B.: Optimum design and analysis of bell crank lever for an automobile. In: Advanced Manufacturing Systems and Innovative Product Design, pp. 189–2086. Springer, Singapore (2021)
5. Urtekin, L.; Özerkan, H.B.; Cogun, C.; Genc, A.; Esen, Z.; Bozkurt, F.: Experimental investigation on wire electric discharge machining of biodegradable AZ91 Mg alloy. J. Mater. Eng. Perform. **30**(10), 7752–7761 (2021)
6. Ramanathan, A.; Krishnan, P.K.; Muraliraja, R.: A review on the production of metal matrix composites through stir casting–Furnace design, properties, challenges, and research opportunities. J. Manuf. Process. **42**, 213–245 (2019)
7. Parthiban, K.; Lakshmanan, P.; Gnanavelbabu, A.: Experimental and theoretical yield strength of silicon carbide and hexagonal boron nitride Reinforced Mg-Zn Nanocomposites Produced by the Combined Effects of Ultrasonication and Squeeze Casting. Silicon. (2022). https://doi.org/10.1007/s12633-022-01679-7
8. Abbas, A.; Rajagopal, V.; Huang, S.J.: Magnesium metal matrix composites and their applications. In: Magnesium Alloys. IntechOpen, London (2021)
9. Emadi, P.; Andilab, B.; Ravindran, C.: Engineering lightweight aluminum and magnesium alloys for a sustainable future. J. Indian Inst. Sci. (2022). https://doi.org/10.1007/s41745-021-00267-9
10. Saranu, R.K.; Chanamala, R.; Putti, S.R.; Mallarapu, G.K.: Investigation of microstructures, mechanical properties of az91e hybrid composite reinforced with silicon carbide and fly Ash. SILICON **13**(7), 2145–2156 (2021)
11. Deng, K.K., et al.: Effect of submicron size SiC particulates on microstructure and mechanical properties of AZ91 magnesium matrix composites. J. Alloy. Compd. **504**(2), 542–547 (2010)
12. Mao, H.; Bai, X.; Wang, Y.; Xu, H.; Hou, J.; Wei, L.; Misra, R.D.K.: Microstructures and high-temperature properties (2022)
13. Yang, Q.; Yan, Z.; Lv, S.; Guan, K.; Qiu, X.: Abnormal creep stress exponents in a high-pressure die casting Mg–Al− RE alloy. Mater. Sci. Eng. A **831**, 142203 (2022)
14. Sameer Kumar, D.; Suman, K.N.S.; Poddar, P.: A study on the impact and fatigue failure of AZ91E–Ni coated alumina composites. Can. Metall. Quart. **59**(3), 316–323 (2020)
15. Zeng, D.; Liu, Z.; Zou, L.; Wu, H.: Tribological behavior of Al2O3-MoO2-SiO2 composite ceramic coating on Al-Zn-Mg-Cu alloy. Coatings **11**(8), 915 (2021)
16. Chen, H.; Alpas, A.T.: Sliding wear map for the magnesium alloy Mg-9Al-0.9 Zn (AZ91). Wear **246**(1–2), 106–116 (2000)
17. Aung, N.N.; Zhou, W.; Lim, L.E.: Wear behaviour of AZ91D alloy at low sliding speeds. Wear **265**(5–6), 780–786 (2008)
18. Lim, C.Y.H.; Lim, S.C.; Gupta, M.: Wear behaviour of SiCp-reinforced magnesium matrix composites. Wear **255**(1–6), 629–637 (2003)
19. Lim, C.Y.H.; Leo, D.K.; Ang, J.J.S.; Gupta, M.: Wear of magnesium composites reinforced with nano-sized alumina particulates. Wear **259**(1–6), 620–625 (2005)
20. Asl, K.M.; Masoudi, A.; Khomamizadeh, F.: The effect of different rare earth elements content on microstructure, mechanical and wear behavior of Mg–Al–Zn alloy. Mater. Sci. Eng. A **527**(7–8), 2027–2035 (2010)
21. Jang, I.J.; Jang, Y.B.; Shin, H.S.; Shin, N.R.; Kim, S.K.; Yu, M.J.; Cho, S.J.: Preparation and characterization of Lanthanum hexaaluminate granule for catalytic application in aerospace technology. In: Proceedings of the 18th International Conference on Composite Materials, pp. 21–26. Jeju, Korea (2011)
22. Gadow, R.; Lischka, M.: Lanthanum hexaaluminate—novel thermal barrier coatings for gas turbine applications—materials and process development. Surf. Coat. Technol. **151**, 392–399 (2002)
23. Sai Ram, Y.N.V.; Tarasasanka, C.; Prabakaran, J.: Preparation and characterization of lanthanum hexa aluminate powders for high temperature application. Mater. Today Proc. **39**, 1472–1475 (2021)
24. Yellapragada, N.V.S.R., et al.: Estimation of lattice strain in lanthanum hexa aluminate nanoparticles using X-ray peak profile analysis. Rev. Rev. Compos. Matér. Av. (2021). https://doi.org/10.18280/rcma.310102

25. Kumar, D.S.; Suman, K.N.S.: Selection of magnesium alloy by MADM methods for automobile wheels. Int. J. Eng. Manuf. **2**, 31–41 (2014)
26. Yano, E.; Tamura, Y.; Motegi, T.; Sato, E.: Effect of carbon powder on grain refinement of an AZ91E magnesium alloy. Mater. Trans. **44**(1), 107–110 (2003)
27. Kant, S.; Verma, A.S.: Stir casting process in particulate aluminium metal matrix composite: a review. Int. J. Mech. Solids **9**(1), 61–69 (2017)
28. Poddar, P.; Srivastava, V.C.; De, P.K.; Sahoo, K.L.: Processing and mechanical properties of SiC reinforced cast magnesium matrix composites by stir casting process. Mater. Sci. Eng. A **460**, 357–364 (2007)
29. Mohapatra, S.K.; Maity, K.: Synthesis and characterisation of hot extruded aluminium-based MMC developed by powder metallurgy route. Inte. J. Mech. Mater. Eng. **12**(1), 1–9 (2017)
30. Sameer, K.D., et al.: Microstructure, mechanical response and fractography of AZ91E/Al2O3 (p) nano composite fabricated by semi solid stir casting method. J. Magn. Alloys (2016). https://doi.org/10.1016/j.jma.2016.11.006
31. Aravindan, S.; Rao, P.V.; Ponappa, K.: Evaluation of physical and mechanical properties of AZ91D/SiC composites by two step stir casting process. J. Magn. Alloys **3**(1), 52–62 (2015)
32. Chelliah, N.M.; Kumar, R.; Singh, H.; Surappa, M.K.: Microstructural evolution of die-cast and homogenized AZ91 Mg-alloys during dry sliding condition. J. Magn. Alloys **5**(1), 35–40 (2017)
33. Poddar, P.; Mukherjee, S.; Sahoo, K.: The microstructure and mechanical properties of SiC reinforced magnesium based composites by rheocasting process. J. Mater. Eng. Perform. **18**, 849–855 (2009). https://doi.org/10.1007/s11665-008-9334-1
34. Hassan, S.F.; Gupta, M.: Development of high performance magnesium nano-composites using nano-Al2O3 as reinforcement. Mater. Sci. Eng. A **392**(1–2), 163–168 (2005)
35. Rahimian, M.; Parvin, N.; Ehsani, N.: Investigation of particle size and amount of alumina on microstructure and mechanical properties of Al matrix composite made by powder metallurgy. Mater. Sci. Eng. A **527**(4–5), 1031–1038 (2010)
36. Qi, Q.-J.: Evaluation of sliding wear behavior of graphite particle-containing magnesium alloy composites. Trans. Nonferrous Met. Soc. China **16**(5), 1135–1140 (2006)
37. Mondal, A.K.; Kumar, S.: Dry sliding wear behaviour of magnesium alloy based hybrid composites in the longitudinal direction. Wear **267**(1–4), 458–466 (2009)
38. Tarasasanka, C.; Ravindra, K.: Application of Taguchi techniques to study dry sliding wear behaviour of magnesium matrix composites reinforced with alumina nano particles. J. Eng. Sci. Technol. **12**(11), 2855–2865 (2017)
39. Dey, A.; Pandey, K.M.: Wear behaviour of Mg alloys and their composites–a review. Int. J. Mater. Res. **109**(11), 1050–1070 (2018)
40. Hutchings, I.M.: Tribology: Friction and Wear of Engineering Materials, 1st edn. Edward Arnold, London (1992)
41. Seyfert, C.: Tribometers, rotational, for sliding wear and friction. In: Mang, T. (Ed.) Encyclopedia of lubricants and lubrication. Springer, Berlin, Heidelberg (2014)